The Plant Cell, Vol. 24: 3823–3837, September 2012, www.plantcell.org

Verticillium Infection Triggers VASCULAR-RELATED NAC DOMAIN7–Dependent de Novo Xylem Formation and Enhances Drought Tolerance in *Arabidopsis*[W]

Michael Reusche,[a] Karin Thole,[a] Dennis Janz,[b] Jekaterina Truskina,[a] Sören Rindfleisch,[a] Christine Drübert,[b,1] Andrea Polle,[b] Volker Lipka,[a,2] and Thomas Teichmann[a]

[a] Department of Plant Cell Biology, Albrecht-von-Haller-Institute, Georg-August-University Göttingen, Julia-Lermontowa-Weg 3, D-37077 Gottingen, Germany

[b] Department of Forest Botany and Tree Physiology, Büsgen-Institute, Georg-August-University Gottingen, Büsgenweg 2, D-37077 Gottingen, Germany

The soilborne fungal plant pathogen *Verticillium longisporum* invades the roots of its *Brassicaceae* hosts and proliferates in the plant vascular system. Typical aboveground symptoms of *Verticillium* infection on *Brassica napus* and *Arabidopsis thaliana* are stunted growth, vein clearing, and leaf chloroses. Here, we provide evidence that vein clearing is caused by pathogen-induced transdifferentiation of chloroplast-containing bundle sheath cells to functional xylem elements. In addition, our findings suggest that reinitiation of cambial activity and transdifferentiation of xylem parenchyma cells results in xylem hyperplasia within the vasculature of *Arabidopsis* leaves, hypocotyls, and roots. The observed de novo xylem formation correlates with *Verticillium*-induced expression of the *VASCULAR-RELATED NAC DOMAIN* (*VND*) transcription factor gene *VND7*. Transgenic *Arabidopsis* plants expressing the chimeric repressor *VND7-SRDX* under control of a *Verticillium* infection-responsive promoter exhibit reduced de novo xylem formation. Interestingly, infected *Arabidopsis* wild-type plants show higher drought stress tolerance compared with noninfected plants, whereas this effect is attenuated by suppression of VND7 activity. Together, our results suggest that *V. longisporum* triggers a tissue-specific developmental plant program that compensates for compromised water transport and enhances the water storage capacity of infected *Brassicaceae* host plants. In conclusion, we provide evidence that this natural plant–fungus pathosystem has conditionally mutualistic features.

INTRODUCTION

The ascomycete *Verticillium* is a soilborne pathogen that colonizes the vascular system of its host plants. Of the five plant pathogenic *Verticillium* species *V. dahliae*, *V. albo-atrum*, *V. tricorpus*, *V. nubilum*, and *V. longisporum* (Klosterman et al., 2009a, 2009b; Inderbitzin et al., 2011), the latter specifically infects cruciferous plants, including the economically important host plant *Brassica napus* and the model plant *Arabidopsis thaliana* (Zeise and von Tiedemann, 2002). Originally considered a long-spored variant of *V. dahliae*, the near-diploid species *V. longisporum* was recently suggested to represent the result of a parasexual hybridization between *V. dahliae* and *V. albo-atrum* and was classified as a species (Karapapa et al., 1997). Despite controversial views on this matter, several recent molecular studies support the taxonomic status of *V. longisporum* as a new *Verticillium* species and the importance of hybrid formation within this genus of phytopathogenic fungi (Klosterman et al., 2009a, 2009b; Collado-Romero et al., 2010; Inderbitzin et al., 2011).

Verticillium persists in the soil in the form of thick-walled, melanized microsclerotia, which germinate in response to root exudates (Mol and van Riessen, 1995). On *B. napus*, *V. longisporum* hyphae first attach to root hairs, proceed to the main root, and grow on the root surface along the junctions of epidermal cells (Eynck et al., 2007). Here, the hyphae directly penetrate without the development of any specific infection structures and grow inter- and intracellularly through the root cortex toward the central cylinder of the root. In the root stele, *Verticillium* enters the xylem cells, proliferates in the vascular system of the root, and at later stages colonizes the xylem of the hypocotyl, stem, and leaf tissue. *V. longisporum* achieves extensive colonization of the whole plant by sporulation within the vascular system, producing conidia that are carried upward with the transpiration stream. Conidia are detained at vessel end walls or bordered pits of individual vessel elements and cross this barrier by building germination tubes that grow into the adjacent vessel cell. During the late stages of plant colonization, *Verticillium* exits the vascular system and starts to feed on senescing stem and leaf tissue. Because of its biphasic life cycle, *Verticillium* is considered a hemibiotroph with a biotrophic life phase within the nutrient-poor environment of the xylem and a necrotrophic phase in the aerial plant tissues.

Colonization of the xylem by pathogenic fungi is often associated with drastic effects on xylem function caused by obstruction of the transpiration stream. In some plants, secreted

[1] Current address: Department of Botany I, Molecular Plant Physiology and Biophysics, Julius-von-Sachs-Platz 2, D-97082 Wuerzburg, Germany.

[2] Address correspondence to vlipka@gwdg.de.

The author responsible for distribution of materials integral to the findings presented in this article in accordance with the policy described in the Instructions for Authors (www.plantcell.org) is: Volker Lipka (vlipka@gwdg.de).

[W] Online version contains Web-only data.

www.plantcell.org/cgi/doi/10.1105/tpc.112.103374

fungal cell wall–degrading enzymes are responsible for clogging of the vessels by formation of vascular gels that originate from plant cell wall components (VanderMolen et al., 1983). In other interactions, the plant actively arrests fungal growth in the xylem by tyloses, which are formed by invagination of the middle lamella from neighboring parenchyma cells through bordered pits (Agrios, 1997). In addition, several fungal toxins with the capacity to induce wilting have been described (Wang et al., 2004; Palmer et al., 2005). Typically, *Verticillium* infections also lead to wilting, with the remarkable exception of *V. longisporum*–infected *Brassicaceae*, which were recently described to maintain their water status (Floerl et al., 2008; Floerl et al., 2010).

To compensate for the effects of a compromised transpiration stream, diseased plants use at least two different strategies. Hop plants tolerant to *V. albo-atrum* infection were reported to show "prolonged or renewed activity" of the secondary cambium, which resulted in newly formed xylem cells that were free of tyloses and fungal mycelium (Talboys, 1958). A different strategy to substitute infected, nonfunctional xylem was described for wilt-resistant carnation (*Dianthus caryophyllus*) plants infected with the vascular pathogen *Fusarium oxysporum* f sp *dianthi*. In this interaction, xylem parenchyma and pith cells adjacent to obstructed xylem were described to undergo renewed cell division and subsequent differentiation into xylem (Baayen, 1986). These two anatomical studies provided early descriptive evidence for pathogen-induced developmental reprogramming of host plant vascular tissues and were interpreted as a compensatory response to maintain functionality. Insight into the underlying molecular machinery is, however, lacking.

The process of cellular dedifferentiation followed by differentiation into cells with a different function is defined as transdifferentiation (Sugimoto et al., 2011). The best-characterized model to study this phenomenon is transdifferentiation of *Zinnia elegans* mesophyll cells to tracheary elements (TEs) (Fukuda and Komamine, 1980). This system facilitated the identification of transdifferentiation phases and allowed isolation and characterization of genes involved in TE differentiation. It was shown that 30 min after initiation of the transdifferentiation process, a NAC transcription factor was upregulated during the early dedifferentiation phase (Milioni et al., 2002). The pivotal role of this class of transcription factors in xylem differentiation was corroborated by microarray analyses of a recently established transdifferentiation system in *Arabidopsis* (Kubo et al., 2005). A group of seven NAC (for NAM, ATAF1/2, and CUC2) transcription factors was identified and designated as VASCULAR-RELATED NAC DOMAIN (VND). Interestingly, overexpression of VND6 and VND7 caused ectopic formation of TEs in leaves and roots of *Arabidopsis* and poplar hybrid aspen (*Populus tremula* × *Populus tremuloides*), indicating a key function of these genes in xylem development. VND6 and VND7 seem to have specific roles, with VND6 regulating metaxylem formation, and VND7 inducing protoxylem development (Kubo et al., 2005).

Our observation that *V. longisporum* infection induces bundle sheath cells to transdifferentiate into TEs prompted us to investigate the phenomenon and molecular basis of pathogen-induced de novo xylem formation in more detail. Moreover, we hypothesized that newly built xylem helps to alleviate the effect of a vascular pathogen on the water status of infected plants. Our results suggest that compromised functionality of vessels that are clogged by fungal activity may be restored by the formation of new xylem elements. Furthermore, we demonstrate a key role for VND6 and VND7 in *V. longisporum*–induced transdifferentiation and show that de novo xylem formation entails enhanced water storage capacity and is accompanied by increased plant drought tolerance.

RESULTS

V. longisporum Infection Induces de Novo Formation of Functional Xylem Elements in *Arabidopsis* and *B. napus*

First, we confirmed by comparative sequence analysis of the ribosomal internal transcribed spacer region (Inderbitzin et al., 2011) that the *Verticillium* isolate used in our studies (VL43; first described in Zeise and von Tiedemann, 2001) belongs to the species *V. longisporum* (see Supplemental Table 1 and Supplemental Figure 1 online). Next, we analyzed in detail *V. longisporum*–induced symptom development on *Arabidopsis* by inoculating ecotype Columbia (Col-0) seedlings using the root-dipping method described below. The infection process was monitored by quantifying fungal DNA in rosette leaves and showed proliferation of the fungus in aerial plant parts (i.e., hypocotyl, petioles, and leaves) at 21 d after inoculation (DAI) (Figure 1A). At 14 DAI, and thus before detection of considerable amounts of fungal DNA, first symptoms typical of *V. longisporum* infection (Floerl et al., 2010), such as stunting and loss of fresh weight, became visible (see Supplemental Figure 2 online). This was also reflected in quantitative analyses, which showed a 56 ± 26% loss in fresh weight and a 61 ± 20% decrease in leaf area at 28 DAI (Figures 1B and 1C). Despite quantitative variation between independent experiments, the leaf area decrease in infected versus control samples was highly consistent (see Supplemental Table 2 and Supplemental Figure 3 online).

In addition to plant stunting and loss of fresh weight, we noticed chlorophyll loss of the tissue directly adjacent to vascular bundles (Figures 1D and 1E), a phenomenon described as vein clearing (Fradin and Thomma, 2006). Microscopic investigation of this phenomenon using trypan blue–stained leaves sampled at 21 DAI showed that chloroplast-containing bundle sheath cells enveloping the vascular bundles in wild-type leaves (Figure 1F, top) were replaced with cells showing secondary cell wall modifications typical of TEs (Figure 1F, bottom; see Supplemental Figure 2 online). Some of these elements exhibited the annular structure characteristics of protoxylem (Figure 1F, bottom), whereas others showed reticulate cell wall fortifications usually seen in metaxylem (Figure 1F, bottom). Subsequent time course analyses suggested that pathogen-induced transdifferentiation of individual bundle sheath cells had occurred between 7 and 14 DAI (see Supplemental Figure 2 online). At 14 DAI, we detected a discontinuous bundle sheath cell layer with interspersed individual xylem cells that exclusively occurred in infected plants, suggesting a pathogen-induced transdifferentiation of individual bundle sheath cells to xylem elements. At later time points of infection, the de novo–formed TEs lined the existing vascular bundle and formed continuous tubes (Figure 1F; see Supplemental Figure 2 online). Comparative cross-section analyses of toluidine blue–

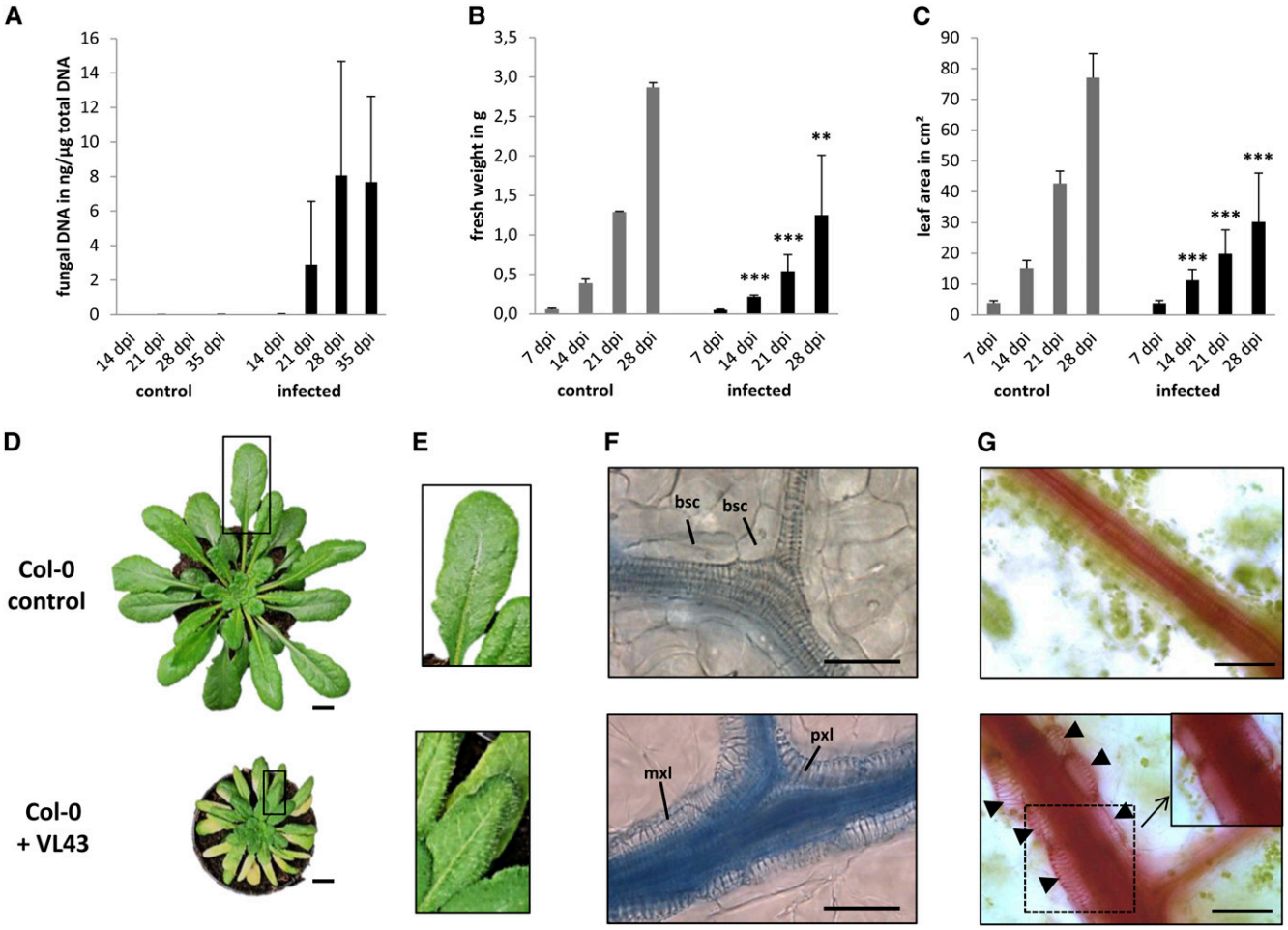

Figure 1. *V. longisporum* Strain VL43 Infection Results in Stunting and Induces Transdifferentiation of Bundle Sheath Cells to Functional TEs.

Arabidopsis Col-0 plants were mock-inoculated with water (control) or incubated in a conidial suspension of VL43 by dipping. Symptom development was analyzed at the indicated time points.

(A) Quantification of fungal DNA in infected plants; data represent means ± SD (n = 3; pools of three plants were analyzed per time point, the experiment was repeated three times, and representative data are shown). dpi, days postinoculation.

(B) Fresh weight of noninfected control and infected plants.

(C) Stunting of infected plants documented by measuring leaf areas.

(B) and **(C)** Data represent means ± SD (n = 18, experiments were repeated three times, and representative data are shown). Significant differences between noninfected control and infected plants at $P \leq 0.01$ and $P \leq 0.001$ are indicated by ** and ***, respectively.

(D) Typical macroscopic phenotype of control and infected plant at 28 DAI. Rectangles designate zoomed-in areas shown in **(E)**.

(E) Vein clearing in leaves of infected plants. Note the yellow appearance of secondary veins in the bottom image. Control (Top) and infected plant (Bottom).

(F) Bright-field microscopy shows bundle sheath cell transdifferentiation at 21 DAI. Leaf vein of noninfected plant (Top) and leaf vein of infected plant (Bottom). Leaves were stained with trypan blue. Note that intensive staining of vascular bundles in the infected plants (Bottom) indicates xylem hyperplasia and is not caused by the presence of fungal hyphae. bsc, bundle sheath cell; mxl, metaxylem-like; pxl, protoxylem-like.

(G) At 21 DAI, leaves were fed with the dye safranin O to show functionality of de novo–formed xylem. Epidermis and mesophyll cells were carefully removed. The inset shows the same area as the dotted box, but with the focal plane set to the lumen of the xylem cells to show staining of xylem sap. Note the tightly associated and chloroplast-containing bundle sheath cells in the noninfected control. Control (Top) and infected plant (Bottom). Arrowheads indicate de novo–formed xylem.

Bars in **(D)** = 1 cm, bars in **(F)** and **(G)** = 50 µm.

stained leaf vascular bundles, hypocotyl, and roots in infected plants and noninfected control plants confirmed considerable anatomical changes in vascular tissues of infected plants (Figures 2A to 2F; see Supplemental Figures 4 and 5 online). In addition to transdifferentiation of leaf bundle sheath cells, we noticed that *V. longisporum* infection induced the formation of a substantially higher number (hyperplasia) of lignified xylem cells within the vascular bundle of leaves (Figures 2B, 2D, and 2F), the hypocotyl xylem, and the central cylinder of roots (see Supplemental Figures 4 and 5 online). The inverse correlation, with

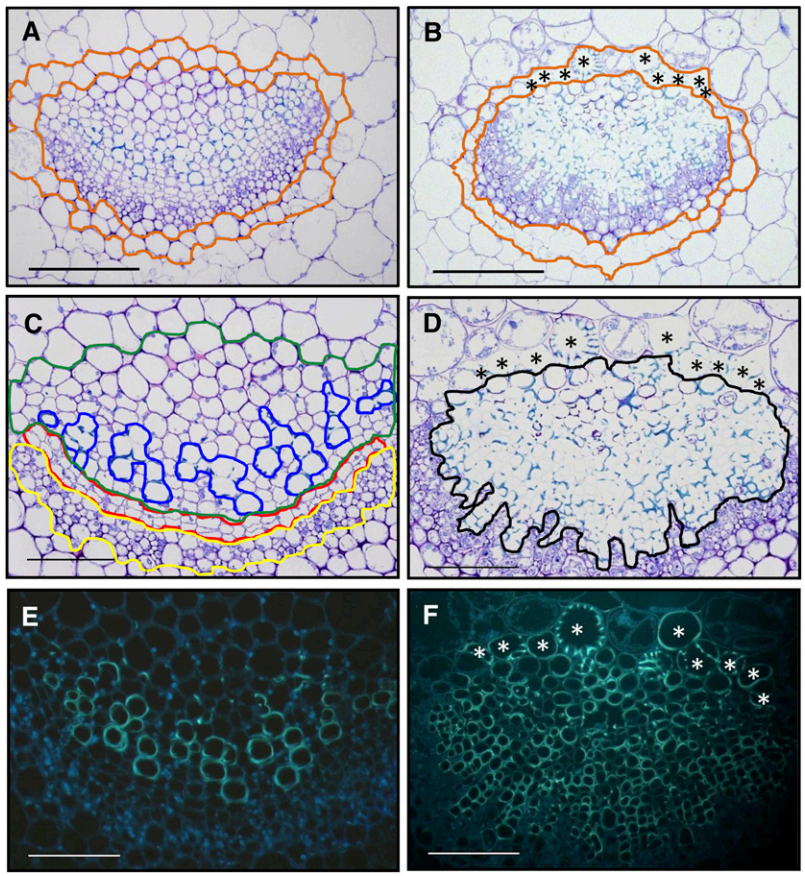

Figure 2. *V. longisporum* Strain VL43 Infection Induces Developmental Changes in Vascular Bundles and Perivascular Cells of *Arabidopsis* Col-0 Plants.

Leaves were harvested 21 DAI from mock-inoculated and VL43-infected plants, and transverse cross-sections of embedded samples were prepared.
(A) to **(D)** Cross-sections for bright-field microscopy were treated with toluidine blue to identify lignified cells, which stain turquoise.
(E) and **(F)** Epifluorescence images that reveal phenolic compounds by autofluorescence. Images show the major leaf vein at the leaf base; **(A)**, **(C)**, and **(E)** are images from noninfected plants, whereas **(B)**, **(D)**, and **(F)** are images from infected plants.
(A) and **(B)** Adaxial bundle sheath cells (localized at the top of the vascular bundle) of infected plants transdifferentiate into xylem. Asterisks indicate transdifferentiated bundle sheath cells; the bundle sheath layer is encircled with ochre lines.
(C) and **(D)** Vascular bundles develop hyperplastic xylem. Cambium (red), phloem (yellow), xylem parenchyma (green), xylem (blue), and hyperplastic xylem (black) are encircled. Asterisks indicate transdifferentiated bundle sheath cells.
(E) and **(F)** Autofluorescence of newly built xylem indicates lignification of TEs; note the continuous radial xylem cell files in **(F)** that indicate origin from increased cambial activity. Asterisks indicate transdifferentiated bundle sheath cells.
Bars = 50 μm.

a dramatic reduction of xylem parenchyma cells and disappearance of the continuous cambial zone in all investigated tissues, suggested that hyperplastic xylem formation was caused by preceding xylem parenchyma cell transdifferentiation and transient reinitiation of cambial activity. The latter conclusion was confirmed by enhanced expression of the cambial marker gene *ARABIDOPSIS THALIANA HOMEOBOX GENE8* (At-*HB8*) (Baima et al., 2001), which in leaves already started at 7 DAI and peaked at 14 DAI (Figure 3A). As a consequence, radial autofluorescent cell files were produced, which distorted the phloem tissue and displaced the vascular tissue borders (Figures 2D and 2F).

Notably, using a transgenic VL43 isolate expressing the β-glucuronidase (GUS) reporter gene, we were able to detect fungal hyphae in the xylem of roots and hypocotyls, but not of leaves at 21 DAI (see Supplemental Figure 6 online). Conceivably, this suggests that de novo xylem formation is not necessarily dependent on in situ fungal colonization and is potentially inducible by a diffusible plant- or pathogen-derived signal that is transported in the transpiration stream.

Next, we tested connectivity and functionality of the newly formed vascular leaf tissue using the safranin O dye method (Freeman and Beattie, 2009). Our experiments confirmed that the new xylem cells formed a continuous conductive system that transported the safranin O dye with the transpiration stream of the leaf (Figure 1G). Together, these results suggested that de novo xylem formation potentially supports water balance maintenance in plants infected with a vascular pathogen.

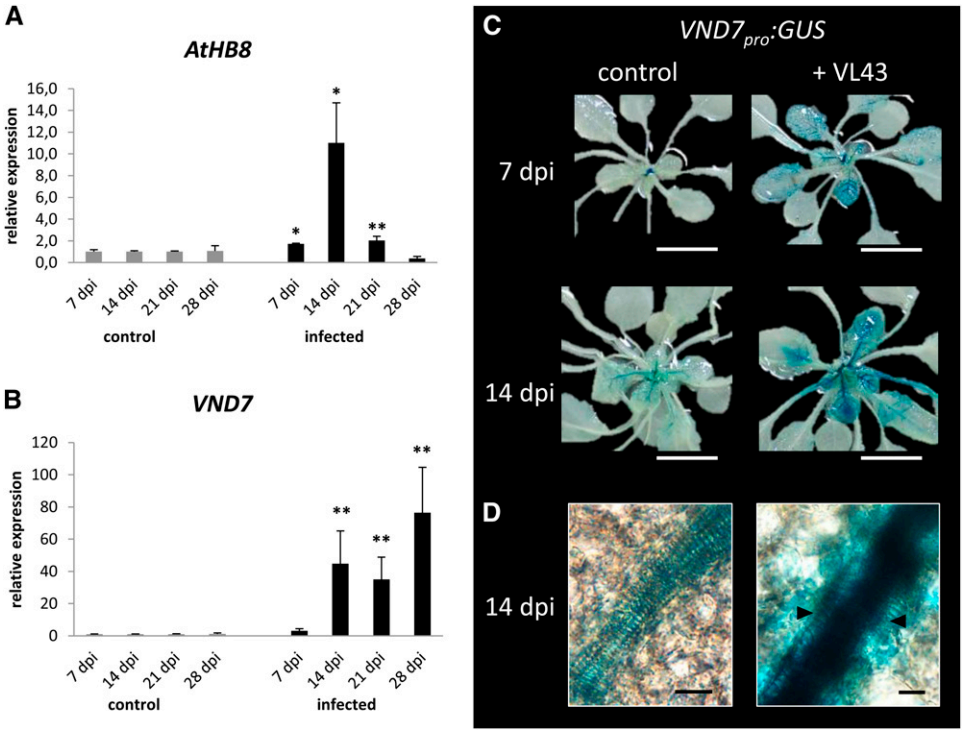

Figure 3. *V. longisporum* Strain VL43 Infection Triggers Increased Cambial Activity and Induces the Expression of the NAC Transcription Factor *VND7* in Bundle Sheath and Vascular Bundle Cells.

(A) Real-time expression analysis of cambial marker At-*HB8* in noninfected control and infected *Arabidopsis* Col-0 plants; data represent means ± SD (n = 3 pools of three plants, the experiment was repeated three times, and representative data are shown); significant differences between noninfected control and infected plants at $P \leq 0.05$ and $P \leq 0.01$ are indicated by * and **, respectively. dpi, days postinoculation.

(B) Real-time expression analyses of *VND7* in noninfected control and infected *Arabidopsis* Col-0 plants (n = 3 pools of three plants, the experiment was repeated three times, and representative data are shown), significant differences between noninfected control and infected plants at $P \leq 0.01$ are indicated by **.

(C) Pattern of $VND7_{pro}$:*GUS* activity in noninfected control (left) and infected plants (right) at 7 and 14 DAI.

(D) Bright-field microscopy shows strong $VND7_{pro}$:*GUS* activity in bundle sheath cells and within the collateral bundle of infected plants at 14 DAI. Arrows indicate recently transdifferentiated bundle sheath cells.

Bars in **(C)** = 1 cm, bars in **(D)** = 10 μm.

To determine whether VL43 induces de novo xylem formation in host plants other than *Arabidopsis*, we analyzed interactions with the agricultural crop *B. napus* (cv *Drakkar*). Indeed, these experiments showed that VL43 infection also induces bundle sheath cell transdifferentiation in this host plant (see Supplemental Figure 7 online), suggesting that developmental reprogramming of vascular bundles might be a general aspect of *V. longisporum* infection biology on its *Brassicaceae* host plants.

V. longisporum–Induced Expression of VND Transcription Factors Correlates with Developmental Reprogramming

Recently, Kubo et al. (2005) identified in the *Arabidopsis* genome seven putative NAC transcription factor genes with homology to a *Z. elegans* NAC transcription factor involved in transdifferentiation and grouped these into the subfamily of *VND* genes. Moreover, the authors showed that within this subfamily, *VND6* and *VND7* are necessary and sufficient for meta- and protoxylem formation, respectively, and that expression of *VND6* and *VND7* depends on the nuclear proteins *ASYMMETRIC LEAVES2-LIKE 19* and *20* (ASL19 and ASL20) in a regulatory feedback loop (Soyano et al., 2008). To elucidate the potential contribution of VND6, VND7, ASL19, and ASL20 for *V. longisporum*–induced developmental reprogramming in leaves, we analyzed their respective expression patterns in pathogen challenge experiments using real-time PCR. Coincident with the start of de novo xylem formation at 14 DAI (see Supplemental Figure 2 online), expression levels of *VND6*, *VND7*, *ASL19*, and *ASL20* were significantly induced (Figure 3B; see Supplemental Figure 8 online). To substantiate our findings, we used $VND7_{pro}$:*GUS* reporter plants (Kubo et al., 2005) in *V. longisporum* infection experiments. Subsequent histochemical analyses confirmed enhanced transcriptional activation of *VND7* in response to VL43 infection and showed strong *VND7* promoter activity in recently transdifferentiated bundle sheath cells and within collateral bundles (Figures 3C and 3D).

V. longisporum–Induced Suppression of VND7 Function in Transgenic *VND7-SRDX* Expressers Reduces de Novo Xylem Formation

Colonization of the xylem by vascular pathogens generally causes water stress in the host plants (Agrios, 1997). We hypothesized that infection-dependent developmental reprogramming may be a compensatory plant response and that suppression of de novo xylem formation might result in enhanced sensitivity to a restricted water supply. Kubo et al. (2005) had previously shown that VND7 fused to the strong repression motif SRDX repressed protoxylem formation in transgenic *Arabidopsis*. Thus, we reasoned that expression of *VND7-SRDX* under control of a *V. longisporum*–inducible promoter with strong activity that parallels the transdifferentiation kinetics may affect de novo xylem formation and would allow us to assess the biological function of the pathogen-induced developmental effects. Recent analyses suggested that the promoter of the *Arabidopsis PEROXIDASE21* (*PER21*) gene meets these criteria (Tappe, 2008). We transformed wild-type *Arabidopsis* Col-0 plants with a $PER21_{pro}$:*VND7-SRDX* construct and selected three independent transgenic lines, L17.7, L18.9, and L22.9, for further studies. Real-time PCR analyses of the transgenic lines confirmed that expression of the *VND7-SRDX* transgene was inducible by VL43 infection in lines L17.7 and L18.9, whereas line L22.9 showed constitutive expression levels of the transgene (Figure 4A; see Supplemental Figures 9B and 9C online). In all three lines, expression of the repressor clearly correlated with dramatically reduced overall de novo xylem formation (12 to 37% of the wild type) in VL43 infection experiments (Figures 4B and 4C; see Supplemental Figures 9A and 10 online). Moreover and consistent with repression of the protoxylem inducer VND7, the few newly formed xylem elements in these transgenics showed a relatively higher proportion of cells with metaxylem morphology (Figure 4D). However, macroscopic disease symptom development was similar in wild-type and transgenic plants and did not indicate significant water status imbalances or wilting of infected suppressor lines (Figure 4B; see Supplemental Figure 9A online).

V. longisporum Infection Increases Drought Tolerance of *Arabidopsis*

We assumed that, under standard watering conditions, plants were still able to maintain a balanced water status and hypothesized that the physiological effects of the newly formed xylem elements might only be unmasked under limiting water supply conditions. Therefore, we conducted drought stress experiments of infected and noninfected plants and monitored the level of drought stress by analysis of leaf area, fresh weight, and water content measurements. Fourteen days after watering of plants was withheld (i.e., 21 DAI) we detected a prominent decrease in leaf area of noninfected control plants, indicating severe drought stress conditions (Figure 5A, left). Unexpectedly, infected wild-type plants exhibited a remarkable macroscopically detectable drought tolerance compared with noninfected wild-type plants (Figure 5B). This observation was also reflected by higher fresh weights and water contents (Figures 5C and 5D).

To monitor whether drought tolerance and increased water content of infected plants correlated with reduced water stress responses, we used the established drought stress reporter lines $RD29B_{pro}$:*GUS* and $AtHB6_{pro}$:*LUC* (Christmann et al., 2005). First, we confirmed that both reporter lines showed wild-type-like disease development (see Supplemental Table 3 and Supplemental Figure 11 online). Subsequent GUS and LUC reporter assays revealed that *Verticillium* infection indeed alleviates drought stress under conditions of restricted water supply (Figures 6A and 6B). This observation was corroborated by the reduced expression of the drought stress marker genes *RESPONSIVE TO DESICCATION29B* (*RD29B*; Christmann et al., 2005), *ARABIDOPSIS NAC DOMAIN CONTAINING PROTEIN72* (*ANAC072*/*RD26*), *DEHYDRATION-RESPONSIVE ELEMENT BINDING PROTEIN2A* (*DREB2A*), and *ARABIDOPSIS THALIANA PHOSPHOLIPASE D DELTA* (*PLD*δ) (Sherameti et al., 2008) in *Verticillium*-infected plants (Figures 6C to 6F).

V. longisporum–Induced Vascular Transdifferentiation and Xylem Hyperplasia Correlates with Improved Drought Stress Tolerance of *Arabidopsis*

Next, to analyze a possible correlation between higher water stress tolerance and pathogen-induced de novo xylem formation, we also studied drought stress responses of the suppressor lines L17.7, L18.9, and L22.9. Indeed, the effect of *Verticillium* infection on water stress tolerance observed in wild-type plants was significantly reduced in these transgenic plants (Figure 5A; see Supplemental Table 4 and Supplemental Figure 12A online). In contrast with wild-type plants, *V. longisporum*–infected transgenic lines showed a decrease in leaf area as well as lower fresh weight and water contents under drought stress conditions (Figures 5A, 5C, and 5D; see Supplemental Table 4 online). The improved water status of infected wild-type plants was reflected by reduced expression of the drought stress marker gene *RD29B* (see Supplemental Figure 12B online). In marked contrast, *RD29B* expression in VL43-infected transgenic suppressor lines was either not reduced or the reduction was less pronounced than in wild-type plants. Finally, we analyzed whether the observed increase in water stress tolerance was caused by reduced transpiration as a consequence of a pathogen-induced decrease in leaf area. To do so, we measured soil water content in a time-course analysis. Our analyses showed the expected soil moisture decrease but did not reveal a difference between infected and noninfected plants (see Supplemental Figures 12C to 12E online). In conclusion, the data support a role of de novo–formed xylem in the increased water stress tolerance of infected plants.

DISCUSSION

Plant–microbe interactions are generally accompanied by dramatic reprogramming of the affected plant tissues that can either serve defense or accommodation (Parniske, 2000; Betsuyaku et al., 2011). Often, and particularly in compatible interactions, this leads to structural and morphological changes or even to the development of new organs. Extrahaustorial or periarbuscular membrane development in individual plant cells, pathogen-induced

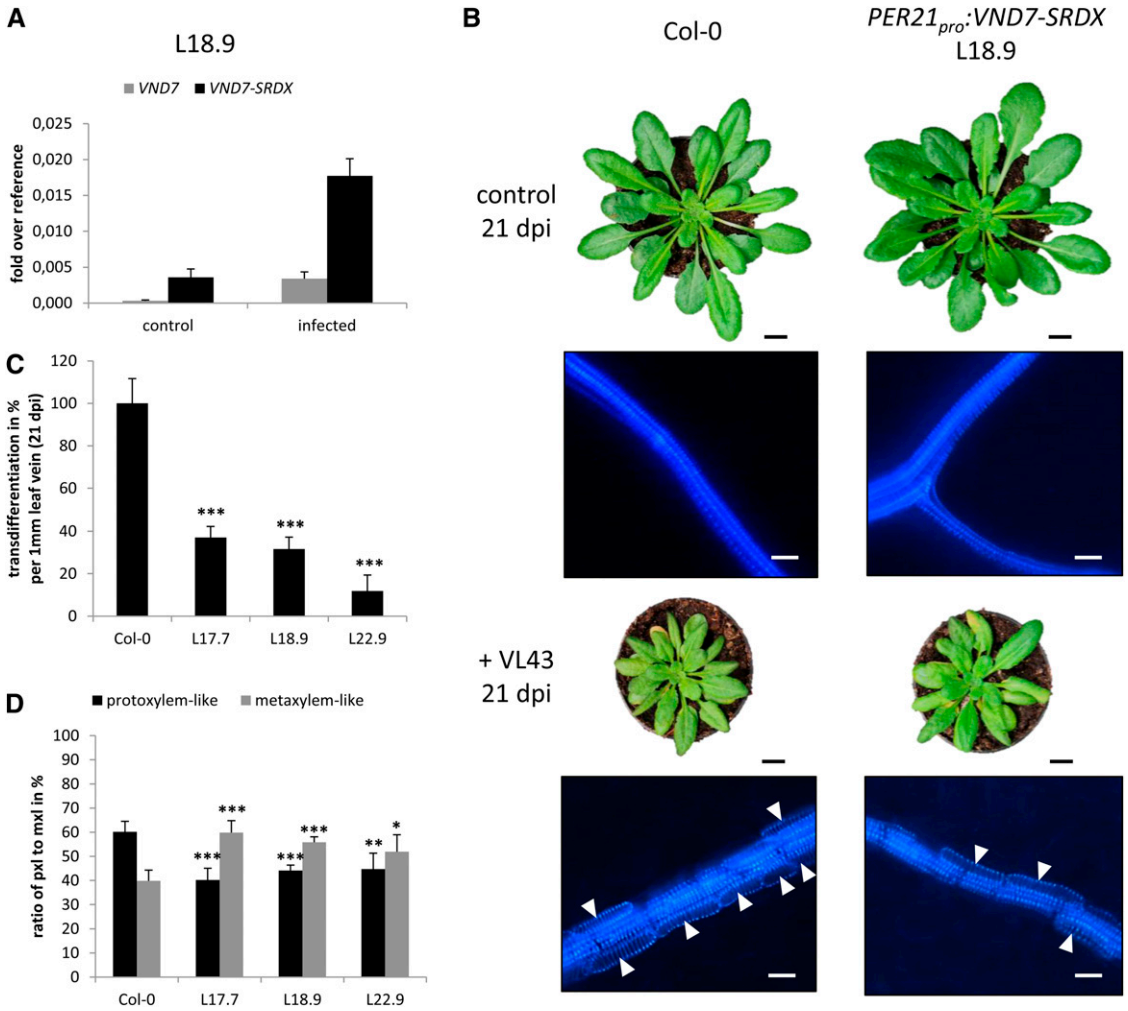

Figure 4. Expression of the Chimeric Suppressor *VND7-SRDX* Reduces the Transdifferentiation Rate in *Arabidopsis*.

Transgenic *Arabidopsis* (Col-0) expressing *VND7-SRDX* under the control of the *Verticillium*-induced *PER21* promoter were generated and analyzed for *Verticillium*-induced transdifferentiation. Wild-type *VND7* and *VND7-SRDX* expression were determined in transgenic plants.

(A) Real-time PCR analysis of *VND7* and *VND7-SRDX* expression at 17 DAI in noninfected control and infected transgenic *VND7-SRDX* expressor plant L18.9; data represent means ± SD (n = 3 plants per time point).

(B) Phenotypes of wild-type Col-0 and the representative transgenic *PER21*$_{pro}$*:VND7-SRDX* line L18.9 under control conditions and upon *Verticillium* infection. Epifluorescence images of corresponding leaf veins are shown (Bottom); arrowheads designate de novo–formed TEs. dpi, days post-inoculation.

(C) Percentage of transdifferentiated bundle sheath cells in infected transgenic *VND7-SRDX* expressor lines compared with infected wild-type Col-0 plants. The number of transdifferentiated bundle sheath cells per millimeter of leaf vein was determined microscopically, and results from wild-type plants were set to 100%. The degree of transdifferentiation in transgenic lines is shown as a percentage of transdifferentiation in wild-type plants. Data represent means ± SD (n = 5 plants, leaves 7 to 10 of each plant were analyzed, and the experiment was repeated twice). Significant differences between wild-type Col-0 and transgenic *PER21*$_{pro}$*:VND7-SRDX* lines at $P \leq 0.001$ are indicated by ***.

(D) The percentage of protoxylem (pxl) and metaxylem (mxl) cells in infected transgenic *VND7-SRDX* expressor and wild-type Col-0 plants. Total number of transdifferentiated cells in wild-type and transgenic plants was set to 100%. Data represent means ± SD (n = 5 plants, 50 cells in leaves 7 to 10 of each plant were analyzed, and the experiment was repeated twice). Significant differences between wild-type Col-0 and transgenic *PER21*$_{pro}$*:VND7-SRDX* lines at $P \leq 0.05$, $P \leq 0.01$ and $P \leq 0.001$ are indicated by *, **, and ***.

Bars in **(B)** = 1 cm for photographs and 25 μm for micrographs.

hypertrophy of plant cell tissues, crown gall tumor formation, and root nodule or syncytium establishment reflect variable degrees of cell specificity and mechanistic complexity.

Here, we show that the vascular pathogen *V. longisporum* triggers distinct intrinsic plant developmental programs that lead to de novo xylem formation and result in enhanced water storage capacity of infected *Arabidopsis* plants. We hypothesize that the observed developmental reprogramming is a plant response to compensate for compromised water transport caused by fungal colonization of the proximal vasculature.

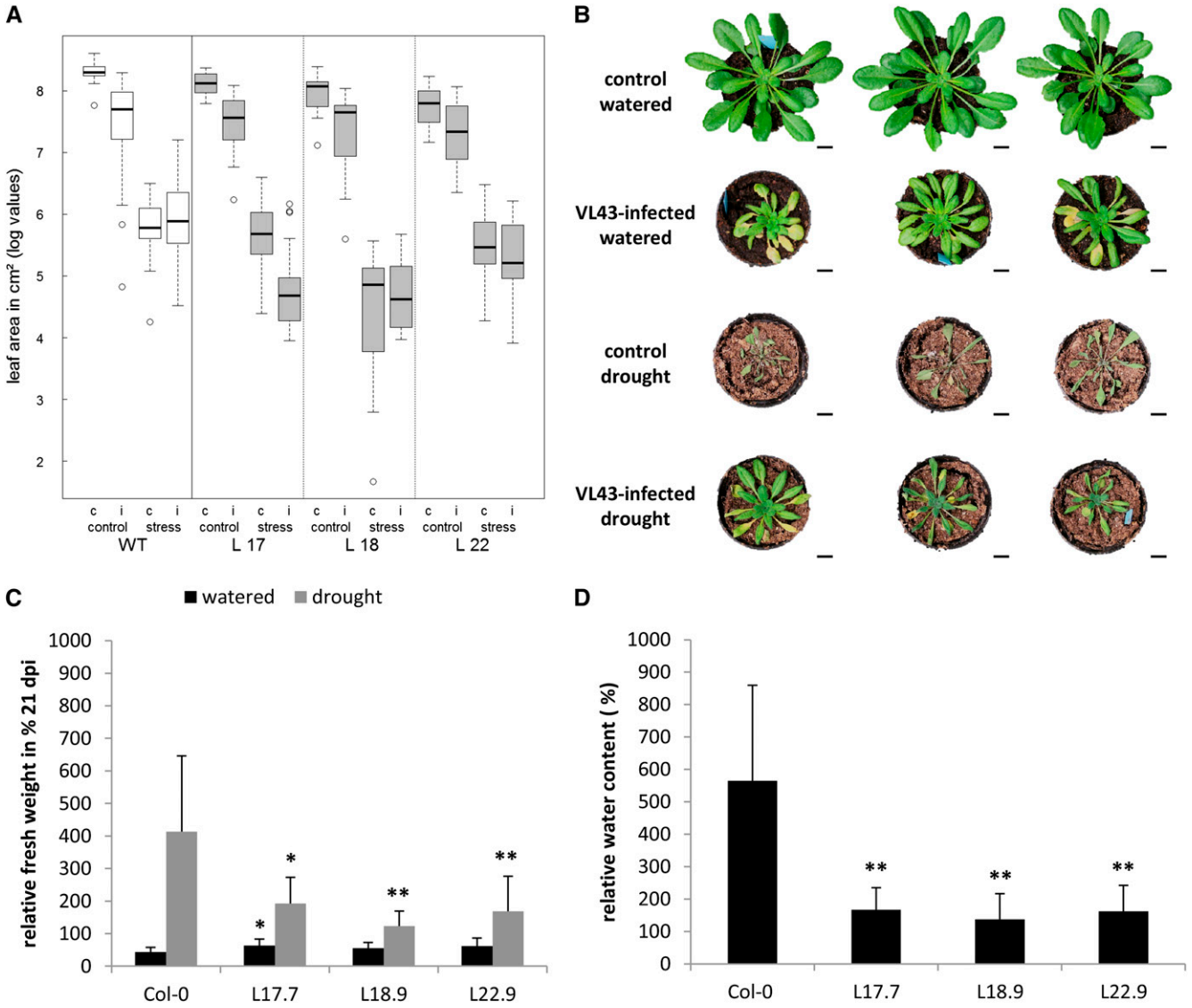

Figure 5. *V. longisporum* Strain VL43–Mediated Increase in Water Content Depends on de Novo Xylem Development and Enhances *Arabidopsis* Col-0 Drought Tolerance.

(A) The figure represents the combined data of three independent experiments which each included wild-type (WT) Col-0 controls and the three transgenic lines L17.7, L18.9, and L22.9. The box plot displays the median of the data set (central bar), the range between the first and third quartile (box), and the highest and lowest values still within the 1.5 interquartile range of the higher and lower quartile, respectively (whiskers). Values outside of this range are depicted as circles. c, noninfected control; i, infected.

(B) Phenotypes of noninfected and infected Col-0 plants at 21 DAI under normal and restricted water supply. Three representative plants are shown for each condition.

(C) Noninfected and infected plants of wild-type Col-0 and three independent transgenic *PER21*$_{pro}$:*VND7-SRDX* lines were exposed to drought stress (watering stopped at 7 DAI). The fresh weight of plants was determined at 21 DAI. The fresh weights of noninfected control plants were set to 100%, and fresh weights of infected plants were calculated in percentages relative to controls. Data represent means ± SD (n = 9, the experiment was repeated three times; representative data are shown). Significant differences between wild-type Col-0 and transgenic *PER21*$_{pro}$:*VND7-SRDX* lines at P ≤ 0.05 and P ≤ 0.01 are indicated by * and **. dpi, days postinoculation.

(D) The noninfected and infected plants of wild-type Col-0 and three independent transgenic *PER21*$_{pro}$:*VND7-SRDX* lines were exposed to drought stress (watering stopped at 7 DAI). The water content of plants was determined gravimetrically at 21 DAI. The water content of noninfected control plants was set to 100%, and the water content of infected plants was calculated as a percentage of the control. Data represent means ± SD (n = 9, the experiment was repeated four times with lines L18.9 and L22.9 and three times with line L17.7; representative data are shown). Significant differences between wild-type Col-0 and transgenic *PER21*$_{pro}$:*VND7-SRDX* lines at P ≤ 0.01 are indicated by **.

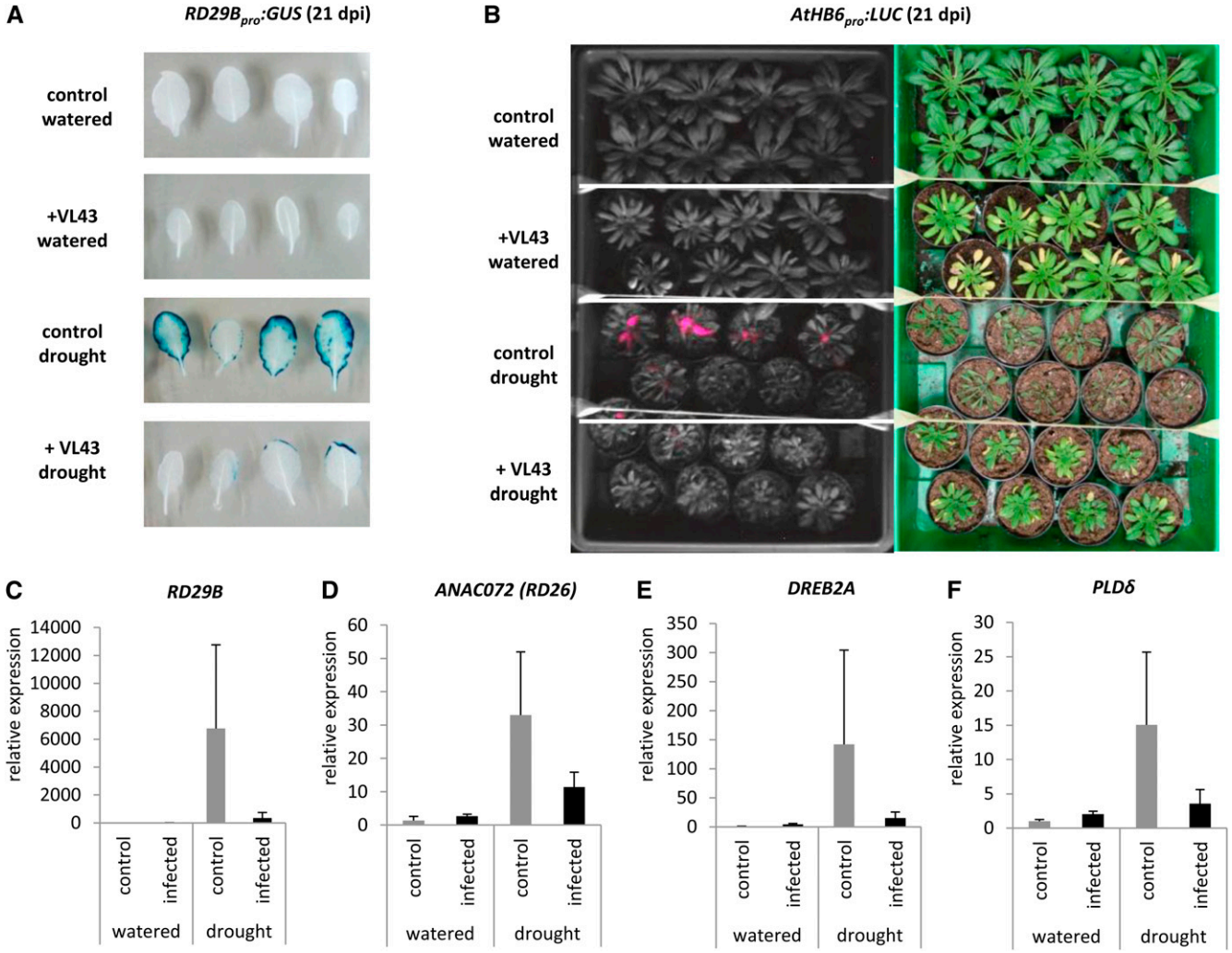

Figure 6. Analyses of Drought Stress Reporter Lines and Drought Stress Marker Genes Reveal Reduced Responsiveness of *V. longisporum* Strain VL43–Infected Plants.

(A) Noninfected control and infected *RD29B*$_{pro}$*:GUS* plants were exposed to drought stress (watering stopped at 7 DAI). Histochemical GUS staining of leaves was done at 21 DAI; the experiment was repeated three times, and representative data are shown.

(B) Noninfected control and infected *ATHB6*$_{pro}$*:LUC* plants were exposed to drought stress (watering stopped at 7 DAI). Luciferase activity in leaves was monitored at 21 DAI (left). Note the lower luciferase activity in infected drought-stressed plants compared with noninfected plants. Macroscopic plant phenotypes are shown on the right. The experiment was repeated two times with similar results. dpi, days postinoculation.

Real-time PCR expression analysis of *RD29B* **(C)**, *ANAC072* **(D)**, *DREB2A* **(E)**, and *PLDδ* **(F)** was performed in noninfected control and infected transgenic Col-0 plants at 17 DAI; data represent means ± SD (n = 3 plants per time point).

V. longisporum Induces Transdifferentiation and Hyperplasia in *Arabidopsis*

We have characterized the effects of systemic *V. longisporum* infection in *Arabidopsis* leaf, hypocotyl, and root tissue and identified two distinct pathogen-induced developmental symptoms: (1) transdifferentiation of bundle sheath and xylem parenchyma cells into xylem cells and (2) vascular hyperplasia caused by enhanced cambial activity.

First, we noticed that the leaf vein–clearing phenomenon typically associated with *Verticillium* infections (Fradin and Thomma, 2006) correlates with transdifferentiation of green, chloroplast-rich bundle sheath cells to novel, functional, and chloroplast-free xylem vessels (Figures 1D to 1G and 2; see Supplemental Figure 2 online). Interestingly, transdifferentiation is restricted to adaxial bundle sheath cells and thus conforms to the typical dorsal polarity of xylem cells in the collateral vascular bundles of *Arabidopsis* leaves (Dinneny and Yanofsky, 2004). Possibly, this suggests that the bundle sheath cells have a fixed positional pattern identity and/or that the transdifferentiation signal originates from the transpiration stream. Bundle sheath cell transdifferentiation is also triggered in *B. napus* (see Supplemental Figure 7 online); therefore, it is conceivable that conserved molecular mechanisms underlie this phenomenon.

Transdifferentiation was originally defined by Okada (1991) as the "irreversible switch of one differentiated cell type into another" and was later extended to correspond to the conversion of one cell type into another (Tosh and Slack, 2002). It is currently debated whether or not this biological process involves a dedifferentiation step before differentiation into the new cell type. Damri et al. (2009) provided a mechanistic model for stress-induced transdifferentiation and hypothesized that the early phase of senescence resembles a dedifferentiated, stem cell–like state. Pathogen-induced senescence may allow cells to dedifferentiate and subsequently transdifferentiate to switch function (Grafi et al., 2011). By contrast, Sugimoto et al. (2010, 2011) recently presented a different view of the developmental steps that lead to transdifferentiation and compared their data with regeneration processes in animals. This group analyzed the regeneration of plants from a variety of tissues via callus formation and concluded that regeneration and transdifferentiation do not involve dedifferentiation to a totipotent stem cell but instead formation of pluripotent cell lineages. Interestingly, Sugimoto et al. (2010, 2011) also provided evidence for the existence of totipotent stem cells surrounding the vasculature of mature aerial *Arabidopsis* organs and argued that plant regeneration originates from these perivascular stem cells. Notably, the identity of these cells remains unknown (Sugimoto et al., 2010, 2011). Future research should examine whether these totipotent cells also contribute to *Verticillium*-induced de novo xylem formation and whether they have a positional and developmental relation to bundle sheath cells.

The best-characterized transdifferentiation system in plants is wound-induced de novo xylem formation, a process that is required for the regeneration of damaged vascular tissues (Sachs, 1981). Interruption of vascular bundles by incision increases the activity of fascicular and interfascicular cambium above and below the wound site and initiates the development of new xylem and phloem elements from the cambium. By contrast, xylem and phloem cells that are formed close to the wound site originate from transdifferentiation of pith parenchyma cells (Nishitani et al., 2002). Finally, vascular elements that originated from parenchyma cells near the wound site connect to the xylem and phloem cells that were built by increased cambial activity of the interrupted vascular bundles, reconstituting the transport of sugars, minerals, and water. The process of wound-induced development of TEs is mimicked in the *Zinnia* in vitro transdifferentiation system. *Zinnia* mesophyll cells transdifferentiate in the presence of auxin and cytokinin into TEs within 72 h. Interestingly, wound-induced transdifferentiation and *Verticillium*-induced transdifferentiation of bundle sheath cells seem to have in common that cells become TEs without previous cell division. As a consequence, the morphology of the transdifferentiated cells resembles that of the original cell, and therefore transdifferentiated bundle sheath cells have an isodiametric outline instead of the elongated tubular appearance of genuine xylem cells (Figures 1F and 1G; see Supplemental Figure 2 online). Thus, our experiments demonstrate that *Verticillium*-induced transdifferentiation of bundle sheath cells represents another rare case of direct transdifferentiation without interposed cell division (Tosh and Slack, 2002).

In addition to transdifferentiation of peripheral bundle sheath cells, we also observed transdifferentiation of leaf xylem parenchyma cells within the genuine collateral vascular bundle, because this cell type was no longer detectable at later infection stages and was positionally replaced by lignified xylem cells (Figures 2D and 2F). This is reminiscent of the de novo xylem formation reported for carnations resistant to *Fusarium* wilt (Baayen, 1986). In this interaction system, nonfunctional xylem was also substituted by transdifferentiation of xylem parenchyma and pith cells into xylem cells, but this transdifferentiation was preceded by cell division.

Importantly, our study also provides evidence that *Verticillium*-induced xylem hyperplasia within the collateral vascular bundle is a consequence of enhanced cambial activity. Hyperplasia is generally defined as an induced increase in cell number and has been reported as a symptom of host plant infection by bacterial, protozoic, root-knot nematode, and fungal plant pathogens (Talboys, 1958; Jammes et al., 2005; Depuydt et al., 2009; Malinowski et al. 2012). Similarly, our analyses showed a dramatic increase of xylem cells within the vascular bundle (Figures 2D and 2F), which is partially caused by transdifferentiation of xylem parenchyma cells. Notably, however, most of the new xylem cells are arranged in radial files, suggesting that they originated from increased cambial activity. This idea is supported by the fact that the cambial activity marker gene At-*HB8* shows an infection-induced expression maximum (Figure 3A), which precedes the observed developmental changes in the leaf. Interestingly, we also detected hyperplastic xylem formation in infected roots and hypocotyls (see Supplemental Figures 4 and 5 online). These findings demonstrate that *V. longisporum* infection generally triggers substantial developmental reprogramming throughout the sequential colonization of belowground and aerial vascular tissues in the *Arabidopsis* plant body. Together, our data corroborate and add molecular support to the early findings of Talboys (1958), who described xylem hyperplasia in *V. albo-atrum*–infected hop and assumed that this was caused by an underlying prolonged or renewed activity of the vascular cambium.

NAC domain transcription factors were recently found to play pivotal roles in both *Zinnia* and *Arabidopsis* transdifferentiation and xylem biogenesis (Demura et al., 2002; Kubo et al., 2005; Yamaguchi et al., 2010); therefore, we analyzed the contribution of this gene family to *Verticillium*-induced developmental reprogramming. Indeed, our data show that *Verticillium*-triggered transdifferentiation of bundle sheath cells depends on NAC transcription factors of the VND family. *VND6* and *VND7* as well as *ASL19* and *ASL20*, encoding nuclear proteins involved in a positive regulatory feedback loop of *VND* gene expression (Soyano et al., 2008), were upregulated within 14 DAI (Figure 3B; see Supplemental Figure 8 online). Suppression of transdifferentiation by a *Verticillium*-induced chimeric VND7-SRDX repressor (Figure 4; see Supplemental Figures 9 and 10 online) corroborated the idea that VND transcription factor activity is required for *V. longisporum*–induced de novo formation of TEs.

Notably, the observed developmental changes were not necessarily dependent on in situ fungal colonization, because fungal hyphae were not detectable in leaf cross-sections (whereas we were able to detect fungal hyphae in roots and hypocotyls at 21 DAI [see Supplemental Figure 6 online]). This suggests that the dark trypan blue staining observed in Figure 1F is caused by dye accumulation in dead hyperplastic leaf xylem cells and that adaxial bundle sheath cell transdifferentiation and xylem

hyperplasia are triggered by a mobile systemic signal released in the *V. longisporum*–colonized proximal vasculature. It remains to be determined whether fungal effector molecules trigger the underlying developmental programs directly or indirectly and which plant hormones are involved.

Pathogen-Induced de Novo Xylem Formation Improves the Water Status of Infected Plants under Drought Stress Conditions

The xylem of plants infected with a vascular pathogen can be severely affected by mycelia, formation of gels, and the response of tissue in the vicinity of vascular bundles. Fungal cultures of *Fusarium* and *V. dahliae* secrete hydrolytic enzymes that have the capacity to degrade components of the plant cell wall. Vander-Molen et al. (1983) reported that a polygalacturonase from *F. oxysporum* f sp *cubense* induced the formation of gels consisting of plant cell wall compounds in xylem vessels of banana (*Musa* spp) and castor bean (*Ricinus communis*). Compounds secreted by *F. o.* f sp *dianthi* stimulate the division of parenchymal cells bordering vascular tissues and finally cause crushing of the vascular bundles (Baayen et al., 1996). Several groups identified *V. dahliae* toxins that induce plant wilting (Wang et al., 2004; Palmer et al., 2005) but did not provide a mechanistic model for toxin activity. These toxins may affect membrane permeability or induce the formation of vascular gels. However, *V. longisporum* infection did not increase membrane permeability in *Arabidopsis* or in oilseed rape (*B. napus*) (Floerl et al. 2008; Floerl et al. 2012). Instead, the water status of infected *Arabidopsis* was increased, and the concentrations of osmolytes were decreased (Floerl et al. 2010). Analyses of Duniway (1971, 1973) on transpirational fluxes in *F. oxysporum*– and *V. dahliae*–infected plants showed increased xylem resistance in the host plants. Together, these data indicate that *Fusarium* and *Verticillium* toxins may cause clogging of vessels without increasing membrane permeability.

As a consequence of vessel clogging, water transport from the soil to transpiring leaves is interrupted. Stomatal closure may counterbalance the restricted water supply for some time, but infected plants will finally begin to wilt. Considering that *V. dahliae* and *V. albo-atrum* also cause wilting symptoms on their respective host plants, it is striking that *V. longisporum*–infected plants do not show any wilting phenotypes but instead exhibit increased water stress tolerance compared with noninfected plants (Figure 5). We substantiated this finding by infection analysis using the drought stress promoter-reporter lines $RD29B_{pro}$:*GUS* and $AtHB6_{pro}$:*LUC* (Figure 6). The promoters of *RD29B* and *ARABIDOPSIS THALIANA HOMEOBOX GENE6* (At-*HB6*) are induced primarily through the abscisic acid–dependent pathway (Himmelbach et al., 2002; Christmann et al., 2005). In line with our conclusion that *V. longisporum* infection alleviates the effects of drought stress in *Arabidopsis*, infected plants generally showed lower $RD29B_{pro}$ and $AtHB6_{pro}$ activity compared with noninfected plants (Figure 6).

The increased drought tolerance of infected plants cannot be explained by the smaller leaf area of infected plants and potentially associated reduced water consumption, because pots of infected and noninfected plants exhibit similar decreases in soil humidity (see Supplemental Figures 12C to 12E online). Suppression of transdifferentiation by *VND-SRDX* expression diminished the *V. longisporum*–mediated effect on drought stress tolerance and, therefore, showed that a prerequisite for increased tolerance is de novo formation of xylem (Figures 5A, 5C, and 5D; see Supplemental Table 4 and Supplemental Figures 12A and 12B online). Functionality of the de novo–formed xylem with respect to water transport was demonstrated by feeding of the water-soluble dye safranin O, because the dye was taken up by the transdifferentiated cells (Figure 1G). Autofluorescence of the newly formed xylem indicates lignification of the secondary cell wall structures (Figure 2F; see Supplemental Figure 5F online). Together, our data fit with recent findings suggesting that cell wall metabolism, production of lignin precursors, and lignification were increased in *V. longisporum*–infected *Arabidopsis* plants (Floerl et al., 2012).

Piriformospora indica, a soilborne, endophytic fungus that was identified in desert plants (Verma et al. 1998), also improves drought tolerance of *Arabidopsis* (Sherameti et al. 2008). *Piriformospora*-colonized plants exposed to severe drought stress exhibited higher fresh weights than noncolonized plants, and photosynthetic activity was less impaired. Moreover, plants protected by *Piriformospora* showed higher survival rates after drought stress treatments. Sherameti et al. (2008) compared expression profiles of colonized and uncolonized *Arabidopsis* and observed a significantly faster and stronger response of the drought stress marker genes *RD29A*, *ANAC072* (*RD26*), *DREB2A*, and *PLD*δ in *Piriformospora*-colonized plants compared with noncolonized plants (it should be noted that *RD29A* and *RD29B*, the latter used in the current study, are both drought- and ABA-responsive genes, although they have slight differences in expression). The authors concluded that *Piriformospora* primes plants to counteract drought stress. Interestingly, *V. longisporum*–infected and drought-stressed *Arabidopsis* showed less severe drought stress symptoms and a reduced expression of the drought stress marker genes *RD29B*, *ANAC072*/*RD26*, *DREB2A*, and *PLD*δ compared with noninfected plants (Figures 6C to 6F). This might indicate that *V. longisporum* infection does not prime plants to drought stress but instead triggers a process that enables plants to avoid osmotic stress by improvement of plant water status under conditions of restricted water supply. Infected drought-stressed plants exhibited higher water contents compared with noninfected plants, and suppression of pathogen-induced de novo xylem formation reduces this protective effect; therefore, we hypothesize that the VL43-induced hyperplasia increases the water storage capacity of leaves. To our knowledge, this phenomenon has only been described for perennial plants so far (Scholz et al., 2008; Betsch et al., 2011).

We conclude from our data that de novo formation of xylem by hyperplasia and transdifferentiation in response to infection of the vascular pathogen *V. longisporum* may be a compensatory plant response resulting in increased plant water storage capacity. Active enhancement of water storage capacity might be advantageous by allowing the plant to resist a combination of biotic, pathogen-induced stress and abiotic drought stress, which likely occur together under natural conditions. Thus, it is tempting to speculate that the *V. longisporum–Arabidopsis* pathosystem represents a conditionally mutualistic interaction that

will allow future in-depth studies to decipher the molecular and evolutionary mechanisms that shape the mutualism–parasitism continuum of plant–microbe interactions in general. Finally, the adaptive plant response we observed is particularly interesting with respect to plant defense strategies in an acceleratingly changing environment (e.g., caused by global warming), and understanding the underlying mechanistic principles might prove useful for engineering drought tolerance in crop plants.

METHODS

Plant Materials and Growth Conditions

Arabidopsis thaliana Col-0 was used as the wild type. *VND7*$_{pro}$*:GUS* (Kubo et al., 2005) was obtained from Taku Demura (RIKEN, Japan). *RD29B*$_{pro}$*:GUS* and *AtHB6*$_{pro}$*:LUC* (Christmann et al., 2005) were provided by Erwin Grill (Technische Universität München, Germany).

Seeds were sown on soil (Fruhstorfer Erde), vernalized at 8°C overnight, and plants were grown under a 8-h light/16-h dark photoperiod at 22/18°C.

Fungal Culture

Verticillium longisporum isolate VL43 was obtained from the Plant Pathology Department, University of Göttingen (Andreas von Tiedemann). A total of 100 μL of a spore suspension (10^6 spores/mL) was cultivated for 1.5 weeks on a rotary shaker at 22°C in the dark in 120 mL of potato dextrose broth (Sigma-Aldrich), supplemented with 0.5 mg/L of cefotaxime. To initiate sporulation, potato dextrose broth was exchanged with Czapek-Dox broth (Sigma-Aldrich) supplemented with 0.5 mg/L of cefotaxime, and cultures were incubated for 1 week. Conidia were harvested by filtration through a folded filter (Schleicher and Schuell 5951/2) and washed two times with sterile water. Spore concentration was determined with a Thoma-Kammer and diluted to a concentration of 10^6 spores/mL for infection.

Inoculation of *Arabidopsis*

For infection experiments on soil, *Arabidopsis* plants (Col-0) were grown in a 1:1 sand/soil mixture (Vitakraft, No. 12262) that was layered on Seramis under a 8-h light/16-h dark photoperiod at 22/18°C. Then, 3.5-week-old plants were incubated for 45 min in a conidial suspension of VL43 (10^6 spores/mL) or mock-inoculated in water by dipping. Plants were transplanted into single pots containing steam-sterilized soil and were kept under a transparent cover for 4 d to ensure high humidity. To monitor infection, the leaf area and fresh weight of the inoculated and control plants were measured at 7, 14, 21, and 28 DAI.

Leaf Surface Measurement

Photographs were taken every week (7, 14, 21, and 28 DAI) with a digital camera and analyzed with custom-made software to quantify the leaf area (Bildanalyseprogramm; Datinf GmbH).

Drought Stress Experiments

Experiments were performed under an 8-h light/16-h dark photoperiod. At 7 DAI, plants were watered until drip-off. Subsequently, control plants were watered normally, whereas watering of plants for drought stress experiments was stopped. Noninfected and infected plants were grown in the same rack. To avoid position effects, racks were regularly turned through 180°, and the position of racks in the climate chamber was swapped.

Calculation of Plant Relative Water Content and Analysis of Soil Humidity

Fresh weight of rosettes was determined using a microbalance (Sartorius). Plants were dried at 65°C in an oven (Thermo), and dry weight was determined immediately after plants were removed from the oven. The water content of noninfected control plants was set to 100%, and that of infected plants was calculated as a percentage of controls. Soil moisture was measured with a moisture meter (Delta-T Devices).

Safranin O Assay

Leaves of plants at 21 DAI were detached at the base of the petiole, and the petiole was immediately placed in an aqueous 1% (w/v) safranin O solution for 2 h (modified from Freeman and Beattie, 2009) to facilitate uptake of the dye into the vascular system. Leaves were briefly washed in water, and the epidermal cell layer and mesophyll cells were carefully removed using forceps and a razorblade to allow observation of the vascular system. Stained xylem was analyzed by brightfield microscopy (Leica DM 5000B).

Histochemical GUS Staining

Whole plants were fixed with cold acetone 90% (v/v) and incubated for 20 min at room temperature. Samples were washed two times for 10 min with washing buffer (50 mM of Na-phosphate buffer, pH 7.2, 10 mM of EDTA, 0.5 mM of ferricyanide, 0.5 mM of ferrocyanide, 0.2% Triton X-100). The washing buffer was exchanged with staining solution (washing buffer + 2 mM of 5-bromo-4-chloro-3-indolyl β-D-glucuronide; Duchefa), and samples were infiltrated in an exsiccator for 30 s, incubated at 37°C overnight, and destained with 98% ethanol.

Trypan Blue Staining

A total of 10 mg of trypan blue (Roth) was dissolved in 40 mL of lactophenol (10 mL of phenol, 10 mL of water, 10 mL of lactic acid, and 10 mL of glycerol) and diluted with 40 mL of 96% ethanol. Leaves were covered with the staining solution in a 50-mL Falcon tube and incubated in a boiling water bath under a fume hood for 2 to 5 min. For destaining, trypan blue solution was exchanged for a chloral hydrate solution (2.5 g/mL), and samples were incubated at room temperature on a rotary shaker overnight. Samples were mounted in 60% glycerol.

Luciferase Measurements

In vivo imaging of luciferase activity was performed by spraying *AtHB6*:*LUC* plants with luciferin (1 mM of D-luciferin potassium salt; Synchem OHG). After 20 min of preincubation in the dark, light emission was assayed for 10 min using a sensitive charge-coupled device camera (C4742-98 water-cooled charge-coupled device camera [Hamamatsu Photonics] with 4 × 4 pixel binning).

Quantification of *V. longisporum* DNA

In planta proliferation of *V. longisporum* was quantified by determining fungal DNA using real-time PCR. Whole rosettes of *Arabidopsis* (Col-0) were used for analyses. Plant tissue was ground in a mortar under liquid nitrogen, and DNA was extracted using the DNeasy Plant Mini Kit (Qiagen). The iCycler System (Bio-Rad) was used to amplify and quantify *V. longisporum* DNA using primers OLG70 (5′-CAGCGAAACGCGATATGTAG-3′) and OLG71 (5′-GGCTTGTAGGGGGTTTAGA-3′) (Eynck et al., 2007). The amplification mix consisted of 1× NH_4 reaction buffer (Bioline), 3 mM of $MgCl_2$, 200 μM of deoxynucleotide triphosphates, 0.4 μM of primers, 0.25 units of BIOTaq DNA polymerase (Bioline), 10 nM of

fluorescein (Bio-Rad), 1:100000 diluted SYBR Green I solution (Cambrex), 20 to 25 ng of template DNA, and double distilled water with a total volume of 25 μL. The PCR program comprised a 2-min denaturation step at 94°C followed by 36 cycles of 20 s at 94°C, 30 s at 59°C, and 40 s at 72°C. The amount of *V. longisporum* DNA was estimated from a calibration curve established with purified fungal DNA.

Real-Time Expression Analysis

RNA was extracted from 50 mg of leaf material using the innuPREP Plant RNA-Kit (Analytik Jena) according to the manufacturer's manual. DNA was digested with DNase I, RNase free (Fermentas). cDNA synthesis from 1 μg of total RNA was performed with the RevertAid H Minus First Strand cDNA Synthesis Kit (Fermentas). The iCycler system (Bio-Rad) was used to amplify and quantify cDNA using primers designed with a tool from Roche. The following primers were used: pPER21-VND7-SRDX (sense 5′-gcttccctgactcgaaggg-3′ and antisense 5′-gggttaagcgaaacccaaac-3′), VND6 (sense 5′-gccatgggacatccaaga-3′ and antisense 5′-tgtggctaaagaaataccattcc-3′), VND7 (sense 5′-cacgaataccgtctccaaaact-3′ and antisense 5′-cctaaatgctcgacacacca-3′), ASL19 (sense 5′-agcgagcaacgtctccaa-3′ and antisense 5′-acggcgtctggtcgtttat-3′), ASL20 (sense 5′-cgtcgctcacatctttgct-3′ and antisense 5′-tgccaaatgggcttgtaagt-3′), RD29B (sense 5′-gaagagtctccacaatcacttgg-3′ and antisense 5′-caactcacttccaccggaat-3′), ANAC072 (sense 5′-acccactcgagctgtacccg-3′ and antisense 5′-ctcgtagccatggaagctcc-3′), DREB2A (sense 5′-ggggtaaatgggttgctgag-3′ and antisense 5′-ttggcaacactgttccccg-3′), PLDδ (sense 5′-cgtggttaaagtgtcaggaagagcc-3′ and antisense 5′-aatcgccatggcgcataccaacc-3′), and At-HB8 (sense 5′-ctcaagagatttcacaacctaacg-3′ and antisense 5′-tcactgcttcgttgaatcctt-3′), and UBQ5 was used for normalization (sense 5′-gacgcttcatctcgtcc-3′ and antisense 5′-gtaaacgtaggtgagtcca-3′). The amplification mix consisted of 1× NH4 reaction buffer (Bioline), 2 mM of $MgCl_2$, 100 μM of deoxynucleotide triphosphates, 0.4 μM of primers, 0.25 units of BIOTaq DNA polymerase (Bioline), 10 nM of fluorescein (Bio-Rad), 1:100000 diluted SYBR Green I solution (Cambrex), 1 μL of a 1:10 dilution of cDNA as template, and double distilled water to a total volume of 25 μL. The PCR regime consisted of an initial 90-s denaturation step at 95°C followed by 40 cycles of 20 s at 95°C, 20 s at 55°C, and 40 s at 72°C. Calculations were done according to the comparative cycle threshold method described by Livak and Schmittgen (2001).

Construction of Transgenic *PER21$_{pro}$:VND7-SRDX* Repression Lines

The *PER21$_{pro}$:VND7-SRDX* construct was ordered from a custom gene synthesis service (GenScript Corporation) and cloned into the binary vector pCambia2300 using *Bam*HI and *Sal*I restriction sites. Transformation of the *Agrobacterium tumefaciens* strain GV3101 carrying the helper plasmid pMP90 was done by electroporation (Bio-Rad, MicroPulser).

Transformation of *Arabidopsis* by Floral Dip

The *Agrobacterium* strain containing the construct *PER21$_{pro}$:VND7-SRDX* was grown on Luria-Bertani plates containing 50 mg/L of kanamycin, 25 mg/L of gentamycin, and 100 mg/L of rifampicin at 28°C for 48 h. A single colony was transferred to 5 mL of DYT medium containing the same antibiotics and was cultured overnight at 28°C with vigorous shaking (180 rpm). The overnight culture was added to 500 mL of the same medium and cultured overnight to an OD_{600} of 0.5 to 1. The *Agrobacterium* cells were harvested by centrifugation for 15 min (4000 rpm, 4°C) and resuspended in infiltration medium (5.0% Suc and 0.05% Silwet L-77). Transformation of *Arabidopsis* plants was performed by the floral dip method (Clough and Bent, 1998). Selection of transgenic plants was performed on selective medium containing kanamycin. Transgenic plants were transferred to soil and grown until seed harvest.

Anatomical Studies

Leaves, hypocotyls, and roots harvested 21 DAI from mock-inoculated and VL43-infected plants were preserved in a mixture of 37% formaldehyde, 100% acetic acid, and 70% ethanol (5:5:90, v/v/v). The entire hypocotyl and a 5 × 5-mm leaf fragment from the adaxial site of the leaf including the midrib were used for embedding. The sample was successively incubated in the following solutions: 70% ethanol for 12 h, 70% ethanol for 2 h, 80% ethanol for 2 h, 90% ethanol for 2 h, 96% ethanol for 2 h, 96% ethanol for 12 h, 100% ethanol for 2 h, 100% ethanol:100% acetone (1:1) for 2 h, 100% acetone for 2 h (two times), acetone:plastic (1:1) for 4 h, acetone:plastic (1:3) for 12 h, and 100% plastic for 12 h (two times). Plastic was a mixture of styrene (Merck) and butyl methacrylate (Sigma-Aldrich) (1:1) containing 2% dibenzoyl peroxide with 50% phthalate (Peroxid Chemie GmbH). The samples were transferred into gelatin capsules (Plano GmbH) and mounted with fresh plastic solution, which was then polymerized at 60°C for 3 d and at 35°C for an additional 10 d. Transverse cross-sections of the embedded samples were obtained with a microtome (Autocut; Reichert-Jung) using freshly produced glass knives (Knifemaker 7800; LKB). The sections were placed on glass slides, which were covered with 0.5% (w/v) gelatin containing 1.77 mM of KCr $(SO_4)_2$ in distilled H_2O. For histochemical analyses, cross-sections were stained with 0.05% toluidine blue in distilled water for 10 min at 60°C, mounted in glycerol, and investigated using bright field microscopy (Axioskop; Zeiss). For detection of autofluorescence, cross-sections were mounted in glycerol and examined with an epifluorescence microscope (Axioskop; Zeiss) using the filter combination G365/FT395/LP420. Photos of autofluorescence were taken with an exposure time of 1.5 s.

Determination of Transdifferentiation Ratios

Leaves (numbers 7, 8, 9, and 10) of short-day–grown plants were harvested at 21 DAI and stained with trypan blue. Transdifferentiated bundle sheath cells were counted along second-order veins (eight consecutive fields of view) and calculated as numbers per 1 mm of vein length. Results obtained with wild-type plants were set to 100% and compared with those obtained with transgenic lines (*PER21$_{pro}$:VND7-SRDX*). In addition, the ratio of protoxylem to metaxylem cells that transdifferentiated from bundle sheath cells was determined by classifying 50 transdifferentiated bundle sheath cells per leaf.

Statistical Analysis

Statistics were evaluated with GraphPad QuickCalcs *t* test (http://graphpad.com/quickcalcs/index.cfm).

Accession Numbers

Sequence information of genes described in this article is filed in the Arabidopsis Genome Initiative database under the following accession numbers: *ANAC072/RD26,* At4g27410; *ASL19*, AT4G00220; *ASL20*, AT2G45420; At-*HB6*, At2g22430; At-*HB8*, At4g32880; *DREB2A,* At5g05410; *PER21*, At2g37130; *PLD*δ, At4g35790; *RD29B*, AT5G52300; UBQ5, AT3G62250; *VND6*, AT5G62380; *VND7*, AT1G71930.

Supplemental Data

The following materials are available in the online version of this article.

Supplemental Figure 1. Comparative Ribosomal Internal Transcribed Spacer Region Sequence Analysis Confirms That Strain VL43 Belongs to the Species *V. longisporum*.

Supplemental Figure 2. *V. longisporum* Strain VL43 Induces Transdifferentiation of Bundle Sheath Cells between 7 and 14 DAI.

Supplemental Figure 3. *V. longisporum* Strain VL43 Reproducibly Induces Stunting of the Host Plant *Arabidopsis* Col-0.

Supplemental Figure 4. *V. longisporum* Strain VL43 Infection Induces Developmental Changes in the Hypocotyl of *Arabidopsis* Col-0 Plants.

Supplemental Figure 5. *V. longisporum* Strain VL43 Infection Induces Developmental Changes in the Root of *Arabidopsis* Col-0 Plants.

Supplemental Figure 6. *V. longisporum* Strain VL43 Proliferates in the Hypocotyl and the Root of *Arabidopsis* Col-0.

Supplemental Figure 7. *V. longisporum* Strain VL43 Induces Transdifferentiation of Leaf Cells in *B. napus* (cv *Drakkar*).

Supplemental Figure 8. *V. longisporum* Strain VL43 Infection Induces Expression of the NAC Transcription Factor *VND6* and the Positive Feedback Loop Regulators *ASL19* and *ASL20* in *Arabidopsis* Col-0 Plants.

Supplemental Figure 9. Expression of the Chimeric Suppressor *VND7-SRDX* Reduces Transdifferentiation Rates in *Arabidopsis*.

Supplemental Figure 10. Expression of the Chimeric Suppressor *VND7-SRDX* Prevents Development of *V. longisporum* Strain VL43–Induced Hyperplasia in *Arabidopsis*.

Supplemental Figure 11. $AtHB6_{pro}$:*LUC* and $RD29B_{pro}$:*GUS* Show Wild-Type Responses to *V. longisporum* Strain VL43 Infection.

Supplemental Figure 12. *V. longisporum* Strain VL43–Mediated Increase of Drought Tolerance Depends on de Novo Xylem Development and Is Not the Consequence of Decreased Water Consumption after *Verticillium* Infection.

Supplemental Table 1. Comparative Ribosomal Internal Transcribed Spacer Region Sequence Analysis Confirmed That Strain VL43 Belongs to the Species *V. longisporum*.

Supplemental Table 2. *V. longisporum* Strain VL43 Reproducibly Induces Stunting of the Host Plant *Arabidopsis* Col-0.

Supplemental Table 3. $AtHB6_{pro}$:*LUC* and $RD29B_{pro}$:*GUS* Show Wild-Type Responses to *V. longisporum* Strain VL43 Infection.

Supplemental Table 4. Expression of the Chimeric Suppressor *VND7-SRDX* Influences the *V. longisporum* Strain VL43–Mediated Increase in Drought Tolerance.

Supplemental Methods 1. Supplemental Methods for the Supplemental Data.

ACKNOWLEDGMENTS

We thank Taku Demura and Arata Yoneda for the *pVND7* constructs and Erwin Grill for $RD29B_{pro}$:*GUS* and $AtHB6_{pro}$:*LUC* constructs. The *Verticillium* "Forschergruppe" (DFG FOR 546) provided valuable comments, suggestions, and materials. In particular, we thank Christiane Gatz, Corinna Thurow, and Hella Tappe for providing information on the *Verticillium*-inducible gene PER21 and the GUS sequence containing plasmid pB9WF9 and Gerhard Braus, Susanna Braus-Stromeyer, and Van Tuan Tran for providing the plasmids pRHN1 and pPK2. We acknowledge Jana Pioch's contribution to the project, Monika Franke-Klein for plant maintenance, and Merle Fastenrath for help with the microscopy of roots. We are grateful for funding by the Deutsche Forschungsgemeinschaft (DFG FOR-546 "Signals in the *Verticillium*-plant interaction"; TE 332/2-1 and Po362/15-1/2).

AUTHOR CONTRIBUTIONS

T.T., A.P., and V.L. designed the experiments. M.R., K.T., J.T., S.R., and C.D. performed the experiments. M.R., K.T., C.D., D.J., A.P., T.T., and V.L. analyzed the data. T.T. and V.L. wrote the article.

Received July 27, 2012; revised August 28, 2012; accepted September 10, 2012; published September 28, 2012.

REFERENCES

Agrios, G.N. (1997). Plant Pathology, 4th ed (San Diego, CA: Academic Press).

Baayen, R.P. (1986). Regeneration of vascular tissues in relation to *Fusarium*-wilt resistance of carnation. Eur. J. Plant Pathol. **92:** 273–285.

Baayen, R.P., Ouellette, G.B., and Rioux, D. (1996). Compartmentalization of decay in carnations resistant to *Fusarium oxysporum f sp dianthi*. Phytopathology **86:** 1018–1031.

Baima, S., Possenti, M., Matteucci, A., Wisman, E., Altamura, M. M., Ruberti, I., and Morelli, G. (2001). The Arabidopsis ATHB-8 HD-zip protein acts as a differentiation-promoting transcription factor of the vascular meristems. Plant Physiol. **126:** 643–655.

Betsch, P., Bonal, D., Breda, N., Montpied, P., Peiffer, M., Tuzet, A., and Granier, A. (2011). Drought effects on water relations in beech: The contribution of exchangeable water reservoirs. Agric. For. Meteorol. **151:** 531–543.

Betsuyaku, S., Sawa, S., and Yamada, M. (2011). The Function of the CLE Peptides in Plant Development and Plant-Microbe Interactions. The Arabidopsis Book **9:** e0149 .10.1199/tab.0149

Christmann, A., Hoffmann, T., Teplova, I., Grill, E., and Müller, A. (2005). Generation of active pools of abscisic acid revealed by in vivo imaging of water-stressed Arabidopsis. Plant Physiol. **137:** 209–219.

Clough, S.J., and Bent, A.F. (1998). Floral dip: A simplified method for *Agrobacterium*-mediated transformation of *Arabidopsis thaliana*. Plant J. **16:** 735–743.

Collado-Romero, M., Jiménez-Díaz, R.M., and Mercado-Blanco, J. (2010). DNA sequence analysis of conserved genes reveals hybridization events that increase genetic diversity in *Verticillium dahliae*. Fungal Biol. **114:** 209–218.

Damri, M., Granot, G., Ben-Meir, H., Avivi, Y., Plaschkes, I., Chalifa-Caspi, V., Wolfson, M., Fraifeld, V., and Grafi, G. (2009). Senescing cells share common features with dedifferentiating cells. Rejuvenation Res. **12:** 435–443.

Demura, T., et al. (2002). Visualization by comprehensive microarray analysis of gene expression programs during transdifferentiation of mesophyll cells into xylem cells. Proc. Natl. Acad. Sci. USA **99:** 15794–15799.

Depuydt, S., Trenkamp, S., Fernie, A.R., Elftieh, S., Renou, J.-P., Vuylsteke, M., Holsters, M., and Vereecke, D. (2009). An integrated genomics approach to define niche establishment by *Rhodococcus fascians*. Plant Physiol. **149:** 1366–1386.

Dinneny, J.R., and Yanofsky, M.F. (2004). Vascular patterning: Xylem or phloem? Curr. Biol. **14:** R112–R114.

Duniway, J.M. (1971). Resistance to water movement in tomato plants infected with *Fusarium*. Nature **230:** 252–253.

Duniway, J.M. (1973). Pathogen-induced changes in host water relations. Phytopathology **63:** 458–466.

Eynck, C., Koopmann, B., Grunewaldt-Stoecker, G., Karlovsky, P., and von Tiedemann, A. (2007). Differential interactions of *Verticillium longisporum* and *V. dahliae* with *Brassica napus* detected with molecular and histological techniques. Eur. J. Plant Pathol. **118:** 259–274.

Floerl, S., Druebert, C., Aroud, H.I., Karlovsky, P., and Polle, A. (2010). Disease symptoms and mineral nutrition in *Arabidopsis thaliana* in response to *Verticillium longisporum* VL43 infection. J. Plant Pathol. **92:** 693–700.

Floerl, S., Druebert, C., Majcherczyk, A., Karlovsky, P., Kües, U., and Polle, A. (2008). Defence reactions in the apoplastic proteome

of oilseed rape (*Brassica napus* var. *napus*) attenuate *Verticillium longisporum* growth but not disease symptoms. BMC Plant Biol. **8:** 129.

Floerl, S., Majcherczyk, A., Possienke, M., Feussner, K., Tappe, H., Gatz, C., Feussner, I., Kües, U., and Polle, A. (2012). *Verticillium longisporum* infection affects the leaf apoplastic proteome, metabolome, and cell wall properties in *Arabidopsis thaliana*. PLoS ONE **7:** e31435.

Fradin, E.F., and Thomma, B.P. (2006). Physiology and molecular aspects of *Verticillium* wilt diseases caused by *V. dahliae* and *V. albo-atrum*. Mol. Plant Pathol. **7:** 71–86.

Freeman, B.C., and Beattie, G.A. (2009). Bacterial growth restriction during host resistance to *Pseudomonas syringae* is associated with leaf water loss and localized cessation of vascular activity in *Arabidopsis thaliana*. Mol. Plant Microbe Interact. **22:** 857–867.

Fukuda, H., and Komamine, A. (1980). Establishment of an experimental system for the study of tracheary element differentiation from single cells isolated from the mesophyll of *Zinnia elegans*. Plant Physiol. **65:** 57–60.

Grafi, G., Chalifa-Caspi, V., Nagar, T., Plaschkes, I., Barak, S., and Ransbotyn, V. (2011). Plant response to stress meets dedifferentiation. Planta **233:** 433–438.

Himmelbach, A., Hoffmann, T., Leube, M., Höhener, B., and Grill, E. (2002). Homeodomain protein ATHB6 is a target of the protein phosphatase ABI1 and regulates hormone responses in *Arabidopsis*. EMBO J. **21:** 3029–3038.

Inderbitzin, P., Davis, R.M., Bostock, R.M., and Subbarao, K.V. (2011). The ascomycete *Verticillium longisporum* is a hybrid and a plant pathogen with an expanded host range. PLoS ONE **6:** e18260.

Jammes, F., Lecomte, P., de Almeida-Engler, J., Bitton, F., Martin-Magniette, M.L., Renou, J.P., Abad, P., and Favery, B. (2005). Genome-wide expression profiling of the host response to root-knot nematode infection in *Arabidopsis*. Plant J. **44:** 447–458.

Karapapa, V.K., Bainbridge, B.W., and Heale, J.B. (1997). Morphological and molecular characterization of *Verticillium longisporum* comb. nov., pathogenic to oilseed rape. Mycol. Res. **101:** 1281–1294.

Klosterman, S.J., et al. (2009a). *Verticillium* comparative genomics: Understanding pathogenicity and diversity. Phytopathology **99:** S65.

Klosterman, S.J., Atallah, Z.K., Vallad, G.E., and Subbarao, K.V. (2009b). Diversity, pathogenicity, and management of *Verticillium* species. Annu. Rev. Phytopathol. **47:** 39–62.

Kubo, M., Udagawa, M., Nishikubo, N., Horiguchi, G., Yamaguchi, M., Ito, J., Mimura, T., Fukuda, H., and Demura, T. (2005). Transcription switches for protoxylem and metaxylem vessel formation. Genes Dev. **19:** 1855–1860.

Livak, K.J., and Schmittgen, T.D. (2001). Analysis of relative gene expression data using real-time quantitative PCR and the 2(-Delta Delta C(T)) Method. Methods **25:** 402–408.

Malinowski, R., Smith, J.A., Fleming, A.J., Scholes, J.D., and Rolfe, S.A. (2012). Gall formation in clubroot-infected *Arabidopsis* results from an increase in existing meristematic activities of the host but is not essential for the completion of the pathogen life cycle. Plant J. **71:** 226–238.

Milioni, D., Sado, P.E., Stacey, N.J., Roberts, K., and McCann, M.C. (2002). Early gene expression associated with the commitment and differentiation of a plant tracheary element is revealed by cDNA-amplified fragment length polymorphism analysis. Plant Cell **14:** 2813–2824.

Mol, L., and van Riessen, H.W. (1995). Effect of plant roots on the germination of microsclerotia of *Verticillium dahliae*. I. Use of root observation boxes to assess differences among crops. Eur. J. Plant Pathol. **101:** 673–678.

Nishitani, C., Demura, T., and Fukuda, H. (2002). Analysis of early processes in wound-induced vascular regeneration using TED3 and ZeHB3 as molecular markers. Plant Cell Physiol. **43:** 79–90.

Okada, T.S. (1991). Transdifferentiation: Flexibility in Cell Differentiation (Oxford, UK: Clarendon Press).

Palmer, C.S., Saleeba, J.A., and Lyon, B.R. (2005). Phytotoxicity on cotton ex-plants of an 18.5 kDa protein from culture filtrates of *Verticillium dahliae*. Physiol. Mol. Plant Pathol. **67:** 308–318.

Parniske, M. (2000). Intracellular accommodation of microbes by plants: A common developmental program for symbiosis and disease? Curr. Opin. Plant Biol. **3:** 320–328.

Sachs, T. (1981). The control of the patterned differentiation of vascular tissues. Adv. Bot. Res. **9:** 151–262.

Scholz, F.C., Bucci, S.J., Goldstein, G., Meinzer, F.C., Franco, A.C., and Miralles-Wilhelm, F. (2008). Temporal dynamics of stem expansion and contraction in savanna trees: Withdrawal and recharge of stored water. Tree Physiol. **28:** 469–480.

Sherameti, I., Tripathi, S., Varma, A., and Oelmüller, R. (2008). The root-colonizing endophyte *Piriformospora indica* confers drought tolerance in *Arabidopsis* by stimulating the expression of drought stress-related genes in leaves. Mol. Plant Microbe Interact. **21:** 799–807.

Soyano, T., Thitamadee, S., Machida, Y., and Chua, N.-H. (2008). ASYMMETRIC LEAVES2-LIKE19/LATERAL ORGAN BOUNDARIES DOMAIN30 and ASL20/LBD18 regulate tracheary element differentiation in *Arabidopsis*. Plant Cell **20:** 3359–3373.

Sugimoto, K., Gordon, S.P., and Meyerowitz, E.M. (2011). Regeneration in plants and animals: Dedifferentiation, transdifferentiation, or just differentiation? Trends Cell Biol. **21:** 212–218.

Sugimoto, K., Jiao, Y., and Meyerowitz, E.M. (2010). *Arabidopsis* regeneration from multiple tissues occurs via a root development pathway. Dev. Cell **18:** 463–471.

Talboys, P.W. (1958). Association of tylosis and hyperplasia of the xylem with vascular association of the hop by *Verticillium albo-atrum*. Trans. Br. Mycol. Soc. **41:** 249–260.

Tappe, H. (2008). *Verticillium longisporum* Induced Gene Expression in *Arabidopsis thaliana*. PhD dissertation. (Göttingen, Germany: Georg-August Universität Göttingen).

Tosh, D., and Slack, J.M.W. (2002). How cells change their phenotype. Nat. Rev. Mol. Cell Biol. **3:** 187–194.

VanderMolen, G.E., Labavitch, J.M., Strand, L.L., and DeVay, J.E. (1983). Pathogen-induced vascular gels: Ethylene as a host intermediate. Physiol. Plant. **59:** 573–580.

Verma, S., Varma, A., Rexer, K.H., Hassel, A., Kost, G., Sarbhoy, A., Bisen, P., Butehorn, B., and Franken, P. (1998). *Piriformospora indica*, gen. et sp. nov., a new root-colonizing fungus. Mycologia **90:** 896–903.

Wang, J.Y., Cai, Y., Gou, J.Y., Mao, Y.B., Xu, Y.H., Jiang, W.H., and Chen, X.Y. (2004). VdNEP, an elicitor from *Verticillium dahliae*, induces cotton plant wilting. Appl. Environ. Microbiol. **70:** 4989–4995.

Yamaguchi, M., Goué, N., Igarashi, H., Ohtani, M., Nakano, Y., Mortimer, J.C., Nishikubo, N., Kubo, M., Katayama, Y., Kakegawa, K., Dupree, P., and Demura, T. (2010). VASCULAR-RELATED NAC-DOMAIN6 and VASCULAR-RELATED NAC-DOMAIN7 effectively induce transdifferentiation into xylem vessel elements under control of an induction system. Plant Physiol. **153:** 906–914.

Zeise, K., and von Tiedemann, A. (2001). Morphological and physiological differentiation among vegetative compatibility groups of *Verticillium dahliae* and *V. longisporum*. J. Phytopathology **149:** 469–475.

Zeise, K., and von Tiedemann, A. (2002). Host specialization among vegetative compatibility groups of *Verticillium dahliae* in relation to *Verticillium longisporum*. J. Phytopathology **150:** 112–119.